

Turbulence Response in the High T_i Discharge of the LHD

Kenji TANAKA, Clive MICHAEL¹⁾, Leonid VYACHESLAVOV²⁾, Hisamichi FUNABA, Masayuki YOKOYAMA, Katsumi IDA, Mikiro YOSHINUMA, Kenichi NAGAOKA, Sadayoshi MURAKAMI³⁾, Arimitsu WAKASA³⁾, Takeshi IDO, Akihiro SHIMIZU, Masaki NISHIURA, Yasuhiko TAKEIRI, Osamu KANEKO, Katsuyoshi TSUMORI, Katsunori IKEDA, Masaki OSAKABE, Kazuo KAWAHATA
and LHD Experiment Group

National Institute for Fusion Science, 322-6 Oroshi-cho, Toki, Gifu 509-5292, Japan

¹⁾*UAEK Fusion Association, Culham Science Center, Oxfordshire OX14 3 DB, United Kingdom*

²⁾*Budker Institute of Nuclear Physics, 630090, Novosibirsk, Russia*

³⁾*Department of Nuclear Engineering, Kyoto University, Kyoto 606-8501, Japan*

(Received 30 December 2009 / Accepted 24 March 2010)

A high ion temperature (T_i) was achieved using a combination of perpendicular and parallel injected neutral beams in the Large Helical Device (LHD). Microturbulence spatial profiles in a high- T_i discharge were measured by two-dimensional phase contrast imaging (2D-PCI) through almost the entire vertical central chord. The 2D-PCI microturbulence spectral ranges covered wavenumbers (k) of 0.1-1 mm⁻¹ and frequencies (f) of 20-500 kHz. The ion thermal conductivity (χ_i) increased in the entire region with increasing T_i . However, the difference between the experimental and neoclassical values of χ_i became smaller at $\rho < 0.5$, where ρ is the normalized position, in the high- T_i phase. Increasing fluctuation was not observed at this location, suggesting improved ion energy transport in this region. On the other hand, at $\rho > 0.5$, χ_i deviated from the neoclassical value due to enhancement of the experimental χ_i and reduction in the neoclassical χ_i by a positive radial electric field. Increasing turbulence was observed at $\rho = 0.6-0.8$, with fluctuations likely propagated to the ion diamagnetic direction in the plasma frame, suggesting that the observed turbulence degrades the ion energy transport at this location in the high- T_i phase.

© 2010 The Japan Society of Plasma Science and Nuclear Fusion Research

Keywords: LHD, turbulence, phase contrast imaging, ion temperature gradient mode, neoclassical transport

DOI: 10.1585/pfr.5.S2053

1. Introduction

Achieving high ion temperature (T_i) is crucial to realizing a magnetic fusion reactor. Therefore, it is pivotal to understand the physical mechanisms governing ion energy transport. In the Large Helical Device (LHD), a T_i of 5.6 keV was achieved by high-powered negative- and positive-ion-based neutral beam injection (N-NBI, P-NBI) with carbon pellet injection [1]. The pumping out of carbon ions was also observed simultaneously, suggesting favorable impurity transport characteristics for future reactor operation [2].

In the LHD, the turbulence characteristics in a high- T_i discharge were measured by two-dimensional phase contrast imaging (2-D PCI) [3] and compared with the characteristics of ion energy transport. For accurate estimation of the NBI deposition power, hydrogen plasma without carbon pellet injection is analyzed in this paper, although the achieved T_i was lower than that in shots with carbon pellet injection. In section 2, the ion energy transport of a high- T_i discharge is described in detail. The experimental and

neoclassical χ_i are compared, and the contributions of neoclassical and anomalous transport in the low- and high- T_i phases are discussed. In section 3, the turbulence characteristics of a high- T_i discharge are described, followed by a summary and discussion in section 4.

2. Transport Analysis of High T_i Discharge

Figure 1 is a time trace of a high- T_i discharge. The magnetic configuration was the so-called inward-shifted configuration, in which the magnetic axis position is 3.6 m. The toroidal magnetic field (B_t) was 2.75 T. P-NBI of 5 MW was perpendicularly injected and later, 16 MW N-NBI was parallel injected. The P-NBI was power modulated to exclude background radiation for the charge exchange recombination spectroscopy (CXRS) used to measure ion temperature and plasma rotation. As shown in Fig. 1 (b), the central electron temperature $T_e(0)$ measured by Thomson scattering and the central ion temperature $T_i(0)$ measured by CXRS started to increase when N-NBI began. The line-averaged density ($n_{e,\text{bar}}$) decreased when

author's e-mail: ktanaka@nifs.ac.jp

N-NBI began. Hydrogen was not fueled externally at $t = 1.5$ - 2.5 s; thus, the change in $n_{e,bar}$ is likely caused by a change in the nature of the transport

Figure 2 shows electron density (n_e), electron temperature (T_e), and ion temperature (T_i) profiles at the low- T_i phase ($t = 1.833, 1.84$ s) and the high- T_i phase ($t = 2.233, 2.24$ s). n_e decreased at $\rho < 0.8$ and increased at $\rho > 0.8$, and T_e and T_i increased at all radial locations. In the LHD, T_e is higher than T_i with N-NBI heating at low density ($n_{e,bar} < \sim 2 \times 10^{19} \text{ m}^{-3}$), since N-NBI heats mostly electrons, but as shown in Fig. 2, T_i exceeds T_e at $\rho < 0.4$ in the high- T_i phase. This indicates that the combination of P-NBI and N-NBI heats ions effectively and suggests that ion confinement is improved in this discharge.

Power balance analysis was conducted using the PROCTR code [4], and neoclassical transport coefficients were calculated using the GSRAKE code [5]. In stellarator/heliotron devices, neoclassical transport is strongly af-

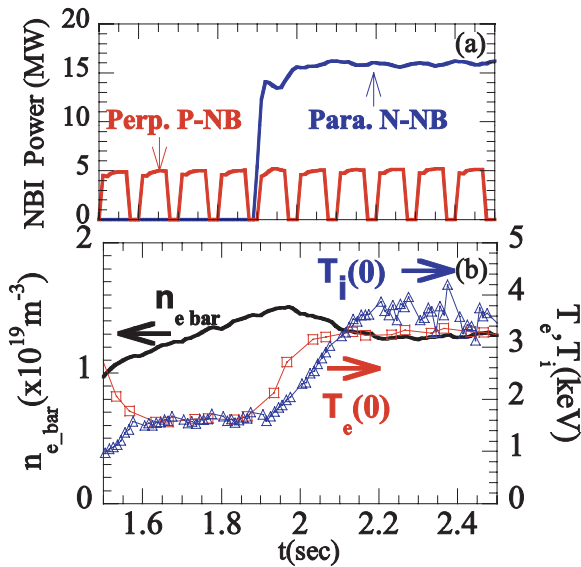


Fig. 1 Time history of (a) NBI injection power, and (b) line averaged n_e , central T_e and T_i .

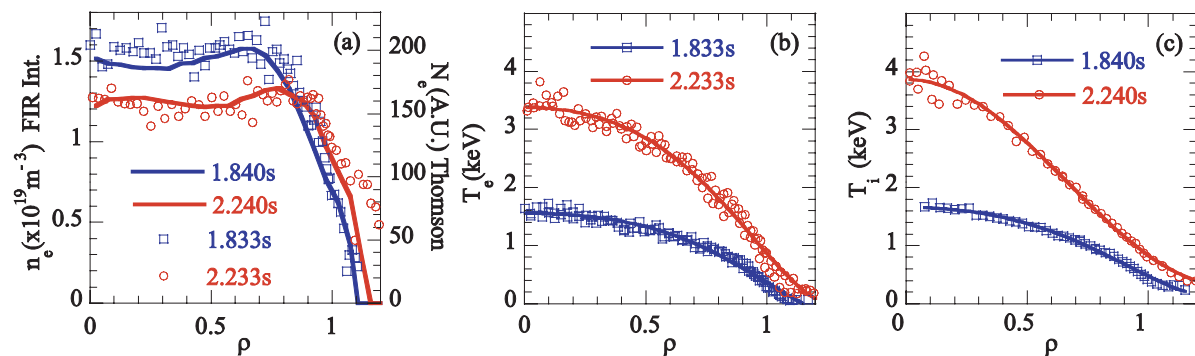


Fig. 2 Profile of (a) n_e , (b) T_e , and (c) T_i at two times indicated in Fig. 1; $t = 1.833, 1.84$ s are at low T_i , and $t = 2.233, 2.4$ s are at high T_i . In Fig. 2 (a) lines and symbols are from the interferometer and Thomson scattering.

ected by the radial electric field (E_r). This is evident in the low-collisionality regime, where neoclassical transport is reduced or enhanced depending on whether E_r is positive or negative. According to the neoclassical theory, E_r changes from negative to positive with increasing T_e under constant n_e [6]. Transition regimes appear between positive and negative E_r where the polarity of E_r is not well determined. Thus, experimental information on E_r is necessary to determine the neoclassical transport in the transition regime.

Figure 3 shows the neoclassical E_r profile predicted by GSRAKE with measured n_e , T_e , and T_i profiles and the experimentally obtained E_r with the use of CXRS. E_r is estimated from the poloidal rotation velocity multiplied by B_t (2.75 T). Toroidal rotation velocities are not included because their contribution is small. Local measurements of E_r were possible at $\rho > 0.7$ and $\rho > 0.8$ in the low- and high- T_i phases, respectively. This limitation is due to the path integral effects of the measurements.

As shown in Fig. 3 (a), at $t = 1.833$ s in the low- T_i phase, E_r is predicted to be negative at $\rho < 1.0$ by GSRAKE. This is partly confirmed by CXRS measurements at $0.7 < \rho < 1.0$, as shown in Fig. 3 (b). On the other hand, at $t = 2.233$ s in the high- T_i phase, theoretically E_r is negative at $\rho < 0.5$, but both positive and negative E_r are theoretically possible at $\rho = 0.5$ - 1.0 , as shown in Fig. 3 (a). The measured E_r is positive, and its value is comparable to neoclassical values at $\rho = 0.8$ - 1.0 in the high- T_i phase. Thus, it is likely that E_r is positive at $\rho > 0.5$, and a reduction in neoclassical transport is expected in this region in the high- T_i phase.

Figure 4 compares neoclassical and experimental values of χ_i in the low- and high- T_i phases. As shown in Fig. 4 (a), at $t = 1.833$ s in the low- T_i phase, the experimental values of χ_i are larger than the neoclassical ones by a factor of two to an order of one. As shown in Fig. 4 (b), at $t = 2.233$ s in the high- T_i phase, two values of neoclassical χ_i are theoretically possible at $\rho = 0.5$ - 1.0 . Higher and lower values correspond to negative and positive E_r , respectively. However, as described above, reduced con-

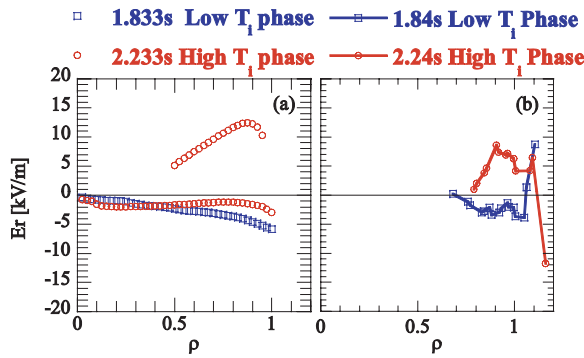


Fig. 3 (a) Neoclassical and (b) experimental radial electric field at low T_i ($t = 1.833, 1.84$ s) and high T_i ($t = 2.233, 2.4$ s).

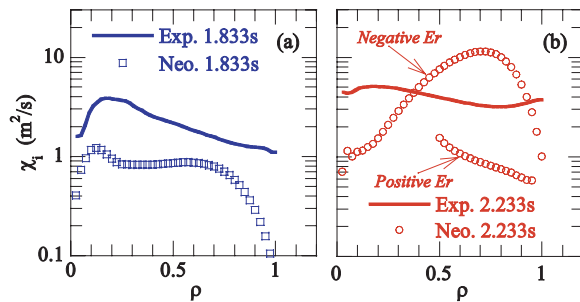


Fig. 4 Experimental and neoclassical χ_i at (a) low T_i ($t = 1.833$ s) and (b) high T_i ($t = 2.233$ s).

Table 1 Comparison of ion and electron thermal conductivities at low T_i ($t = 1.833$ s) and high T_i ($t = 2.233$ s).

	Low T_i $\rho=0.2-0.4$ $t=1.833$ s	Low T_i $\rho=0.6-0.8$ $t=1.833$ s	High T_i $\rho=0.2-0.4$ $t=2.333$ s	High T_i $\rho=0.6-0.8$ $t=2.333$ s
$\chi_{i \text{ exp.}} (\text{m}^2/\text{s})$	3.22	1.56	4.78	3.33
$\chi_{i \text{ neo.}} (\text{m}^2/\text{s})$	0.85	0.76	3.05	0.90
$\chi_{i \text{ exp.}}/\chi_{i \text{ neo.}}$	3.80	2.04	1.57	3.70

ductivities with positive E_r are likely at this location, since the measured E_r was positive at $\rho = 0.8-1.0$.

The comparisons of neoclassical and experimental χ_i values are summarized in Table 1. The averaged values at $\rho = 0.2-0.4$ and $\rho = 0.6-0.8$ are compared. The former represents the core region, where E_r is negative at high T_i , and is selected for stable analysis of the power balance for a nonzero gradient. The latter represents the edge region, where E_r is positive at high T_i , and is selected because of the clear difference in the nature of the fluctuations, described in the next section.

As shown in Table 1, at $\rho = 0.2-0.4$, the ratio of experimental to neoclassical χ_i decreased from 3.80 in the low- T_i phase to 1.57 in the high- T_i phase. At $\rho = 0.6-0.8$, it increased from 2.04 in the low- T_i phase to 3.70 in the high- T_i phase. The contribution of anomalous ion energy transport decreased by a factor of about 2.4 in the core re-

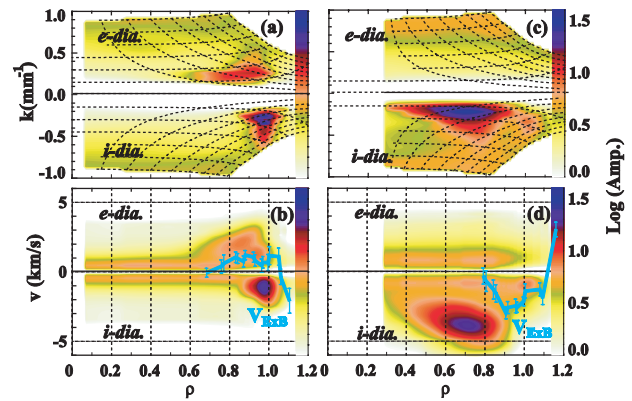


Fig. 5 Spatial profile of k (a), (c), and phase velocity in the laboratory frame (b), (d) at $t = 1.8-1.85$ s (low T_i) and $t = 2.2-2.25$ s (high T_i). e-dia. and i-dia. indicate the electron and ion diamagnetic directions in the laboratory frame, respectively.

gion ($\rho = 0.2-0.4$) and increased by a factor of about 1.8 in the edge region ($\rho = 0.6-0.8$).

3. Turbulence Characteristics of High T_i Discharge

The turbulence of a high- T_i discharge was measured with a sampling frequency of 1 MHz. The fluctuation spectrum is broad, indicating turbulent fluctuations. Frequencies of 20-500 kHz and wavenumber components of 0.1-1.0 mm⁻¹ were analyzed.

Figure 5 shows spatial profiles of the k spectrum and the phase velocity of the fluctuation measured by 2D-PCI at low T_i ($t = 1.8-1.85$ s) and high T_i ($t = 2.2-2.25$ s). In Figs. 5 (a) and (c), the grid marked by dotted lines indicates the approximate resolutions in wavenumber and normalized plasma radius [3]. The measured k is dominated by poloidal components; thus, the propagation directions of the fluctuations are associated with the electron diamagnetic direction (e-dia.) or ion diamagnetic direction (i-dia.) in the laboratory frame (lab. frame). The $E_r \times B_t$ poloidal rotation velocities measured with CXRS are shown in Figs. 5 (b) and (d). The propagation directions of the fluctuations in the plasma frame are identified by comparison with the plasma poloidal $E_r \times B_t$ rotation.

As shown in Figs. 5 (a) and (b), at $t = 1.8-1.85$ s in the low- T_i phase, the fluctuation is localized at $\rho = 0.7-1.0$. One peak at $\rho = 0.8$ propagates to the e-dia. direction in the lab. frame, the other peak, at $\rho = 1.0$, propagates to the i-dia. direction in the lab. frame. Compared with the poloidal rotation velocity, both peaks propagate in the e-dia. and i-dia. direction in the plasma frame as well. Velocity shear from the e-dia. to i-dia. direction at this location is widely observed in N-NBI heated plasmas [7]. The normalized k values of these peaks ($k\rho_i$, where ρ_i is the ion Larmor radius) are around 0.26.

At $t = 2.2-2.25$ s in the high- T_i phase, the fluctuation

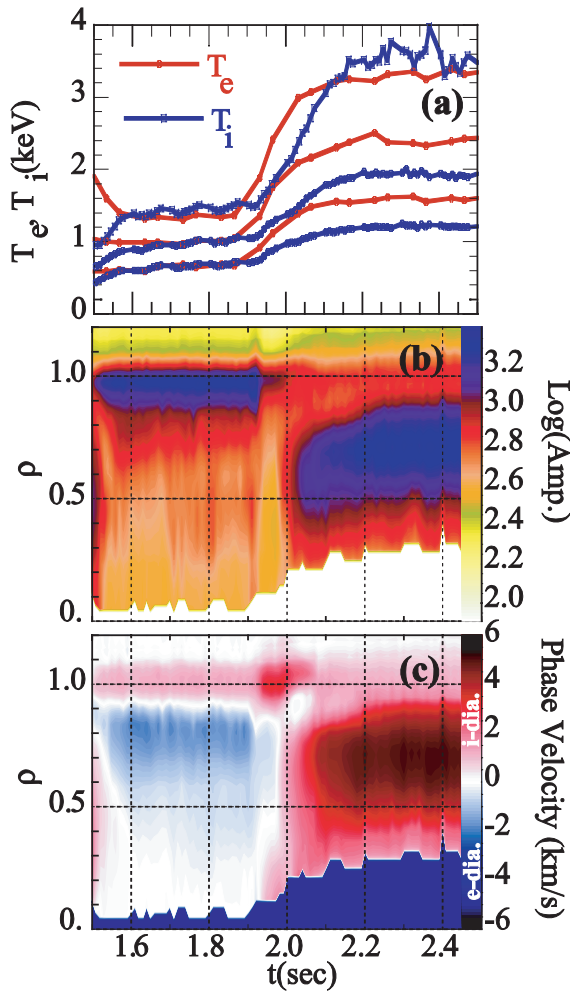


Fig. 6 Time history of (a) T_e and T_i , (b) the fluctuation amplitude, and (c) the fluctuation phase velocity in the laboratory frame. In (a), the radial locations of T_e and T_i are $\rho = 0.3, 0.7$, and 0.9 from the upper trace. White and dark blue regions in (b) and (c) indicate regions inaccessible to measurement.

in the spatial profiles changed dramatically. As shown in Figs. 5 (c) and (d), the fluctuation at $\rho = 0.8-1.0$ decreased, and instead, the fluctuation increased at $\rho = 0.6-0.8$. The value of $k\rho_i$ at $\rho = 0.6-0.8$ was around 0.45. The poloidal rotation velocity measured by CXRS was around zero at $\rho = 0.8$, as shown in Fig. 5 (d). On the other hand, the phase velocity at $\rho = 0.8$ was 3.9 km/s in the i-dia. direction. Therefore, it is likely that the fluctuation at $\rho = 0.6-0.8$ propagates to the i-dia. direction in the plasma frame.

Figure 6 shows the time history of T_i , T_e , the fluctuation amplitude, and its phase velocity. The fluctuation at $\rho = 0.8-1.0$ decreased when T_e and T_i started to increase at 1.9 s. On the other hand, the fluctuations at $\rho = 0.6-0.8$ started to increase at $t = 2.0$ s when T_i was increasing and T_e had almost stopped increasing. The increase in fluctuation at $\rho = 0.6-0.8$ coincides with the T_i increase rather than the T_e increase. This suggests that the driving term of the turbulence at $\rho = 0.6-0.8$ is T_i or the T_i gradient.

4. Discussion and Summary

The ion temperature increased with increasing NBI power and could be associated with improved confinement. As described in section 2, the contribution of anomalous transport is different in the central region ($\rho < 0.5$) and the outer region ($\rho > 0.5$) in the low- and high- T_i phases.

The reduction in the anomalous contribution at $\rho < 0.5$ in the high- T_i phase likely helped make it possible to achieve high T_i . In this location, no clear fluctuation peak was observed, as shown in Figs. 5 (c) and (d). This suggests that turbulence is stable or stabilized in this location.

At $\rho > 0.5$, the radial electric field changes from a negative value in the low- T_i phase to a positive value in the high- T_i phase. This is predicted by GSRAKE and partly confirmed by CXRS measurements. Because of this transition in E_r , the neoclassical χ_i value stays almost constant in the high- T_i phase compared with values in the low- T_i phase. The experimental χ_i value increased in the high- T_i phase; consequently, the anomalous ion transport contribution increased.

The fluctuation increased at $\rho = 0.6-0.8$ in the high- T_i phase, where the anomalous ion transport contribution increased. This suggests that the observed fluctuation plays a role in ion energy transport. The measured fluctuation at $\rho = 0.6-0.8$ in the high- T_i phase most likely propagates in the i-dia. direction in the plasma frame. This fluctuation increased with increasing T_i or T_i gradient. The observed peak value of $k\rho_i = 0.45$ at $\rho = 0.6-0.8$ was comparable with the theoretical prediction at $\rho = 0.6$, which is $k\rho_i = 0.3$, from a nonlinear gyrokinetic simulation of the ion temperature gradient (ITG) for the modeled profile [8]. Thus, the observed fluctuation at $\rho = 0.6-0.8$ in the high- T_i phase shows the characteristics of ITG turbulence. However, a detailed comparison with gyrokinetic linear and nonlinear simulations and a more precise parameter dependence will be necessary to identify the observed turbulence in the high- T_i phase.

The reduction in turbulence at $\rho = 0.8-1.0$ is not clearly linked to transport. As shown in Fig. 4, χ_i is dominated by anomalous transport in both the low- and high- T_i phases. The electron density at $\rho = 0.9-1.05$ increased in the high- T_i phase, as shown in Fig. 2 (a), but the H_α intensity also increased. Thus, it is not clear if particle confinement at $\rho = 0.8-1.0$ is improved in the high- T_i phase.

For further understanding, it is necessary to compare the experimental and neoclassical transport coefficients and turbulence characteristics at different heating powers and different magnetic axis positions, which will reveal different transport characteristics. Also, measurements of E_r in the entire region are absolutely essential to confirm the results described here.

- [1] O. Kaneko *et al.*, Plasma Fusion Res. **4**, 027 (2009).
- [2] K. Ida *et al.*, Phys. Plasmas **16**, 056111 (2009).
- [3] K. Tanaka, C. Michael, L. N. Vyacheslavov *et al.*, Rev. Sci. Instrum. **79**, 10E702 (2008).

-
- [4] H. C. Howe, 1993 *Proctr nid user and numerical guide* Oak Ridge, Tennessee 37831 Oak ridge national laboratory.
- [5] C. D. Beidler and W. N. G. Hitchon, *Plasma Phys. Control. Fusion* **36**, 317 (1994).
- [6] H. E. Mynick and W. N. G. Hitchon, *Nucl. Fusion* **23**, 1053 (1983).
- [7] K. Tanaka *et al.*, *Fusion Sci. Tech.* **51**, 97 (2007).
- [8] T. H. Watanabe *et al.*, *Nucl. Fusion* **47**, 1383 (2007).